Cations distribution by Rietveld refinement and magnetic properties of MgCrxFe2−xO4 spinel ferrites

S. Ouyahia[1], A. Rais[2], B. Bozzo[3], K. Taibi[1] & A. Addou[2]

1 Laboratory of Materials Science and Engineering, USTHB,

Algiers, Algeria

2 Laboratory of Science and Technical Environment and Valorization, Department of Process Engineering,

University Abdelhamid Ibn Badis of Mostaganem, Mostaganem 27000, Algeria

3 Institut de Ciencia de Materials de Barcelona-CSIC, Carrer dels Til-lers, Campus UAB, 08193 Bellaterra, Spain

Abstract

Magnesium–chromium ferrites MgCrxFe2−xO4 ($0 \le x \le 1$) were studied using X-ray diffraction and magnetization measurements. Rietveld refinement of XRD patterns confirmed the cubic spinel structure in the space group Fd-3m and enabled to obtain the cations' distribution amongst octahedral and tetrahedral sites of this structure. Magnetization measurements were performed using vibrating sample magnetometer (VSM) in the temperature range of 300–700 K and superconducting quantum interference device (SQUID) in the range of 10–300 K. Hysteresis loops for each concentration x at 300 K, show non-linear variation of saturation magnetization (MS) with chromium content. Both coercitive field and remanence decrease with increasing chromium content. MS variations with temperature indicate that the Curie temperature TC decreases with increasing chromium content. On the basis of Néel's two sub-lattice crystal field model, the cations' distribution enabled to calculate the theoretical magnetic moments at 0 K which are compared and discussed with those extracted by extrapolation to 0 K from MS experimental data.

Introduction

The magnetic properties of spinel ferrites are known to depend on the cation types and their distribution among the interstitial sites of the spinel lattice [1,2,3,4]. It is common to write their general formula like (M1−δFeδ) [MδFe2−δ] O4, where δ represents the degree of inversion, the round and square brackets denote the tetrahedral (A) and octahedral [B] interstitial sites, respectively. The A and B sites of the FCC lattice formed by O2− anions are occupied by the divalent metal cation M and the trivalent Fe3+ cation. There are three kinds of spinel structures depending on the value of δ which is the fraction of the A-sites occupied by Fe3+ cation; the structure is a normal spinel if $\delta = 0$, it is an inverse spinel if $\delta = 1$; and it is a partially inverse spinel if $0 < \delta < 1$ [5]. On the other hand, the distribution of cations depends mainly on the processing parameters of the preparation method; for example, varying the sintering temperature in the ceramic technique or

varying the calcination temperature in the sol–gel auto-combustion technique will change the distribution [6,7,8,9]. Spinel structure ferrites have brought considerable interest because of their remarkable electrical and magnetic properties in many technological applications, such as magnetic storage systems, magnetic resonance imaging and many others [10,11,12,13,14,15].

Furthermore, $MgFe_2O_4$ is a soft magnetic and semiconducting material whose cations' distribution is a direct function of processing parameters and the earlier reported results of this system reveal that Mg^{2+} ions exist in both sites but have preference for octahedral sites [16, 17]; hence, magnesium ferrites are well known to be a partially inverse spinel structure whose degree of inversion δ depends entirely on the preparation method [18]. Since the magnetic moment of Mg^{2+} is zero, the magnetic coupling in $MgFe_2O_4$ originates from the magnetic moment of Fe cations of both A and B sites pointing in opposite directions which lead to a weaker net moment than any of the sub-lattices. Thus, due to this partial inversion of the spinel structure, the magnetic anisotropy in $MgFe_2O_4$ is among the lowest than any of the other spinel ferrites [19].

In the last decade, several researchers have doped $MgFe_2O_4$ by various trivalent cations (e.g. Cr^{3+}, Al^{3+}, Ga^{3+}) to substitute iron and studied the structural, vibrational and magnetic properties of the mixed ferrites [20,21,22]. Subsequently, understanding thoroughly how magnetic properties of these ferrites are linked with the cationic distribution would enable to fine-tune these properties by regulating the distribution. It is well known that chromium substitutions in any spinel ferrites have preference to octahedral sites only [23, 24]. So, in the case of magnesium ferrites, choosing chromium for doping would yield to lowering the degree of inversion δ and, hence, varying the net magnetic moment of this system in one way or the other. In other words, this would tailor the magnetic parameters according to the needs of a broad range of technological applications.

This work is a continuation on the same spinel ferrite system ($MgCr_xFe_{2-x}O_4$) whose structural and vibrational properties have been reported in our earlier publication [25]. In this article, the magnetic properties of chromium-doped magnesium spinel ferrites are studied in relationship with their cations' distribution obtained by Rietveld refinement. As far as we are aware, no theoretical and experimental studies of the magnetic properties of $MgCr_xFe_{2-x}O_4$ ferrites at both low and high temperatures have been reported.

Experimental

Five samples of the ferrite system Mg $Cr_xFe_{2-x}O_4$ at compositions of x = 0, 0.2, 0.4, 0.7 and 1, were prepared by the conventional double-sintering ceramic technique. The starting materials were analytical reagent-grade MgO, Fe_2O_3 and Cr_2O_3 (BDH) and were weighed stoichiometrically as per chemical formula unit. The details of samples preparation are described in previous publication [26]. The single-phase spinel structure was confirmed by the X-ray diffraction spectra (XRD) of these samples obtained with a PANalytical X'Pert Pro diffractometer using CuKα radiation (i = 1.5406 Å).

The magnetization measurements in the temperature range of 300 K to 700 K were performed using the vibrating sample magnetometer (VSM) of 10−5 emu sensitivity (Microsense EZ9 brand). The

magnetic field ranged from 0 to ± 22 kOe. In the temperature range of 10 K to 300 K, magnetizations were measured using the superconducting quantum device (SQUID) of 10−7 emu sensitivity within a longitudinal field range of 0 to 70 kOe (Quantum Design brand, MPMS-XL7 model). The two instruments (VSM and SQUID) were calibrated at 300 K using a 99.99% pure nickel sample with a standard magnetization value of MS = 54.9 emu/g.

Results and discussion

Rietveld refinement and cation distribution

All XRD patterns were analyzed using HighScore Plus® program (produced by PANalytical B.V. under license number 10003977) based on the Rietveld refinement method [27]. The refinement of all XRD patterns for MgCrxFe2−xO4 (x = 0, 0.2, 0.5, 0.7 and 1) ferrites was indexed to peaks in space group Fd3m with planes: (220), (311), (222), (400), (422), (511), (440), (620), (533), (622), (444), (551), (553) and (644), thus proving the formation of single-phase cubic spinel structure [20]. Note that the reflection peaks of pure Mg ferrite are consistent with those reported for MgFe2O4 (JCPDS Card No. 86-2267). A representative refined spectrum of MgFe2O4 is illustrated in Fig. 1.

Fig. 1

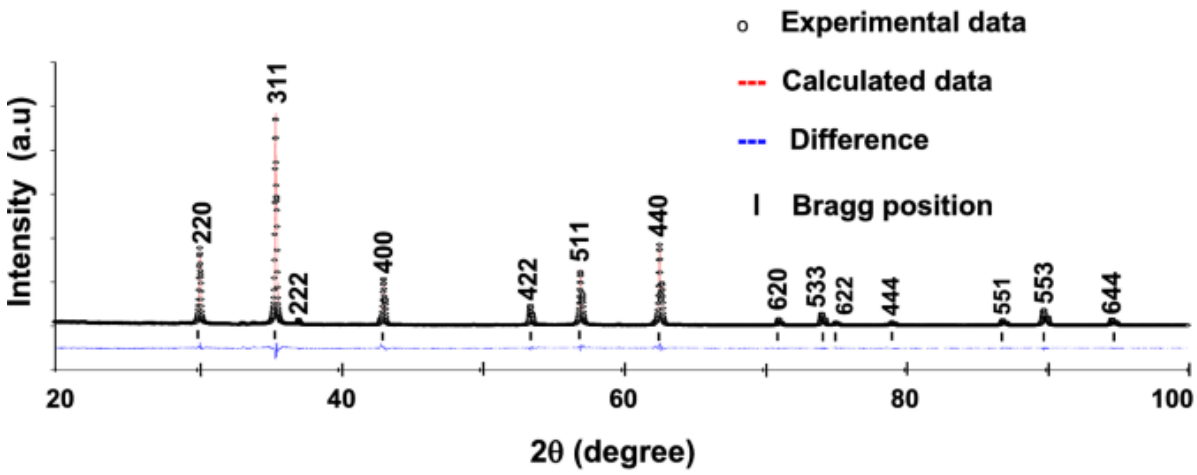

Rietveld refined XRD pattern of MgFe2O4

To model the XRD patterns peak profile, a pseudo-Voigt function was utilized with the oxygen positions (x = y = z = u) taken as free parameters. However, all other atomic fractional positions were taken as fixed parameters, others, such as lattice constants, peak shapes and site occupancies, were taken as free parameters. The typical fractional atomic positions (x = y = z) of the cations and oxygen position parameter u are given in Table 1. The quality of Rietveld fittings was assessed using the reliability R-factors expected and weighted profile Rexp and Rwp, respectively, that must be less than 10%. The goodness-of-fit GoF = Rwp/Rexp and χ2 must tend to one, when these parameters reached their minimum value, the best fit to the experimental diffraction data is achieved [28, 29]. Table 1 shows all these conventional factors. Figure 1 shows experimental and calculated data as well as the difference between the two, thus confirming the reasonably good fit for all compositions [30].

x	Atomic positions			R_{exp} (%)	R_{wp} (%)	GoF	χ^2	S O F (Wyckoff position)				
	Atoms	x = y = z	u					Mg_A (8a)	Fe_A (8a)	Mg_B (16d)	Fe_B (16d)	Cr_B (16d)
0	Mg/Fe	0.375	0.244	6.71	9.61	1.43	2.49	0.138	0.855	0.430	0.569	0.0
	Fe/Mg	0.000										
0.2	Mg/Fe	0.375	0.243	6.53	8.77	1.34	2.34	0.199	0.799	0.396	0.496	0.098
	Fe/Cr/Mg	0.000										
0.5	Mg/Fe	0.375	0.242	7.12	8.48	1.19	2.59	0.261	0.697	0.363	0.4	0.246
	Fe/Cr/Mg	0.000										
0.7	Mg/Fe	0.375	0.242	6.92	8.26	1.18	1.89	0.358	0.628	0.32	0.319	0.352
	Fe/Cr/Mg	0.000										
1	Mg/Fe	0.375	0.241	7.43	9.94	1.33	2.30	0.510	0.456	0.246	0.255	0.481
	Fe/Cr/Mg	0.000										

Table 1 Rietveld refinement conventional factors: fractional atomic positions (x = y = z), oxygen position parameter u, Rietveld fit R-factors, goodness of fit (GoF), χ2 and site occupancy factors (S O F) at tetrahedral (A) and octahedral (B) sites of MgCrxFe2xO4 at chromium content x = 0, 0.2, 0.5, 0.7 and 1

During the refinement, the occupancies of the cations in tetrahedral and octahedral sites are constrained to preserve the stoichiometry of the prepared ferrites. As seen in Table 1, the resulting site occupancy factors (SOF) are calculated so that their sum in A and B sites equals about one. Hence, the stoichiometric coefficients for cations in A sites are equal to the SOF sum, but those of cations in B sites are double of the SOF sum, and this is consistent with the spinel ferrites formula AB2O4 [5, 31]. As such, the cations' distribution was determined using the Rietveld refinement of the occupancy values and is shown in as well as Ni–Al ferrites. From this distribution, one can see that Mg ions are in both tetrahedral and octahedral sites, which reveal that all samples are in partially inversed spinel structure irrespective of the chromium content. However, since the degree of inversion defined as the fraction of Fe3+ in A sites or the stoichiometric coefficient of this cation, one can see that this inversion decreases with chromium content. This is consistent with the decrease of the lattice constant a, as shown in Table 2, with iron substitution by chromium which could be interpreted as due to bigger size effect of Fe3+ (0.67 Å) than Cr3+ (0.64 Å). This has already been discussed in a previous publication on Mg–Cr ferrites [20] and similar behavior has been reported for mixed structure spinel Ni–Cr ferrites [24] as well as Ni–Al ferrites [26].

x	a (Å)	Cations distribution	M_{0K} (μ_B)				
			Theory at 0 K			Experiment at 0 K	
			M_A	M_B	M_{0K}	$T^{3/2}$ law	T^2 Law
0.0	8.386	$(Fe_{0.855}\ Mg_{0.138})\ [Fe_{1.138}\ Mg_{0.860}]\ O_4$	4.3	5.7	1.40	1.25	1.20
0.2	8.380	$(Fe_{0.799}Mg_{0.199})\ [Fe_{0.990}\ Cr_{0.190}\ Mg_{0.790}]\ O_4$	4.0	5.55	1.55	1.36	1.31
0.5	8.376	$(Fe_{0.697}\ Mg_{0.261})\ [Fe_{0.800}\ Cr_{0.492}\ Mg_{0.726}]\ O_4$	3.49	5.48	1.99	1.49	1.44
0.7	8.373	$(Fe_{0.628}\ Mg_{0.358})\ [Fe_{0.638}Mg_{0.640}\ Cr_{0.704}]\ O_4$	3.14	5.30	2.16	1.94	1.87
1	8.369	$(Fe_{0.456}\ Mg_{0.510})\ [Fe_{0.510}\ Cr_{0.962}\ Mg_{0.492}]\ O_4$	2.28	5.44	3.16	2.77	2.68

Round brackets denote A sites. Square brackets denote B sites. Theoretical and experimental magnetic moments M_{oK} (μ_B) per formula unit in Bohr magnetons μ_B. The net theoretical moment $M_{oK} = M_B - M_A$; M_A and M_B are magnetic moments of A and B sub-lattices respectively. The experimental moments are obtained by linear extrapolation to o K of $T^{3/2}$ and T^2 Block function laws

Table 2 Refined lattice parameter a and cations distribution of MgCrxFe2−xO4 obtained from Rietveld refinement of XRD patterns

To simulate a 3-D view of this system spinel structure, we have used CaRlne Crystallography software under License number 030118-4-cc0245. This software needs the refined cell parameter, space group and atomic coordinates (x,y,z) of cations Mg2+, Cr3+, Fe3+ and anion O2−. A representative 3-dimensional view of sample MgCr0.5Fe1.5O4 is shown in Fig. 2. The tetrahedral A site, in which Fe/Mg atom is situated amidst four oxygen atoms which form the corners of a regular tetrahedron and octahedral B sites, where Fe/Cr/Mg atom is situated in the middle of the six oxygen atoms forming the corners of a regular octahedron are clearly shown in the refined crystal structure.

Fig. 2

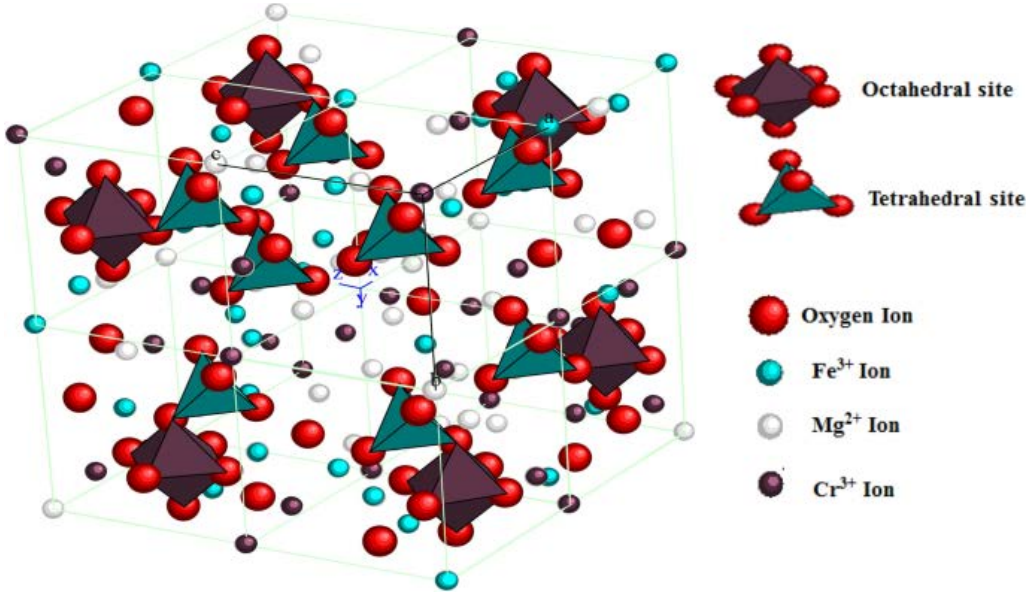

Unit cell 3-D simulation view of ferrite spinel structure of MgCr0.5Fe1.5O4

VSM measurements

The magnetizations versus magnetic field curves at 300 K of all samples are shown in Fig. 3. The magnetic parameters extracted from the Hysteresis loops, i.e. saturation magnetization (MS), coercitive field (HC) and remanence (MR), are listed in Table 3. Our data values are in good agreement with those of Anjum et al. [32] for Cr-substituted Mg ferrites with x = 0 to 0.5 prepared by double-sintering technique. However, it is in less good agreement with those of Hankare et al. [33] nano-ferrite Mg–Cr prepared by co-precipitation method and also less good with Raghasudha et al. [34] prepared by sol–gel auto-combustion method. This again confirms that magnetic parameters of spinel ferrites depend to a large extent on the preparation route [35,36,37,38].

Fig. 3

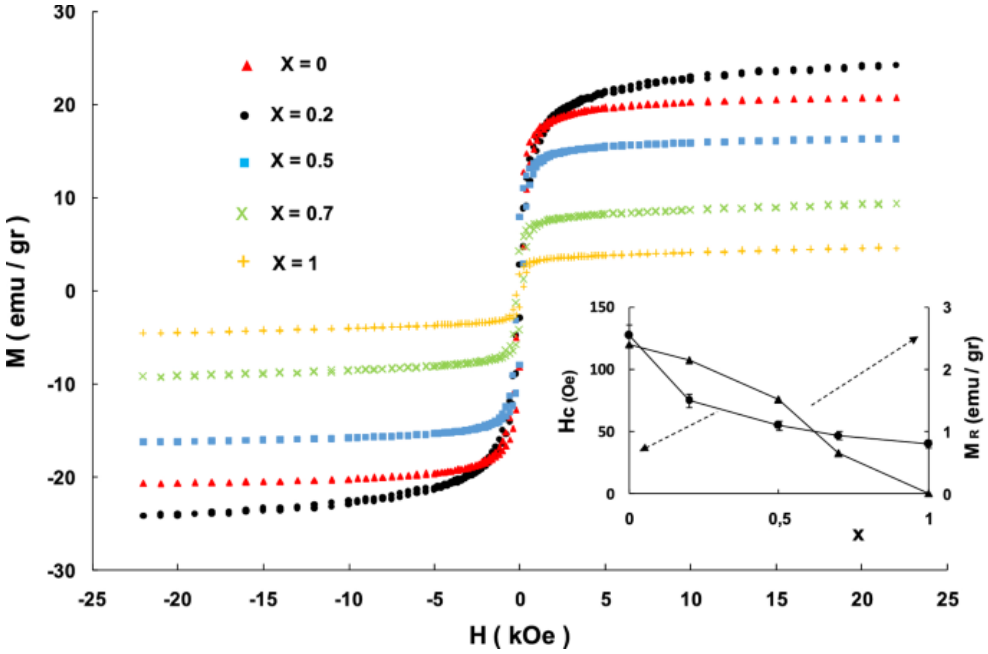

Magnetizations M versus magnetic field H of ferrites Mg CrxFe2−xO4 at 300 K for different chromium content: x = 0, 0.2, 0.5, 0.7 and 1. The inset shows the Coercitive field HC and Remanence MR versus chromium composition x

x	M_S (emu/g)	H_C (Oe)	M_R (emu/g)	T_C (K)
0.0	20.7	127 ± 10	2.4	630
0.2	24.2	75 ± 5	2.1	600
0.5	16.3	55 ± 3	1.5	490
0.7	9.3	47 ± 2	0.65	450
1	4.6	40 ± 2	0.02	350

Table 3 Saturation magnetization MS, coercitive field HC, remanence MR at 300 K of MgCrxFe2xO4 and Curie temperatures TC at chromium content: x = 0, 0.2, 0.5, 0.7, 1

The inset of Fig. 3 shows variations with chromium content of HC and MR. It can be observed that within error bars, HC decreases monotonically with chromium content as well as MR but with significantly less uncertainty. The HC and MR behavior could be explained on the basis of the cations' distribution and the A–B, A–A and B–B sites exchange interactions of the magnetic ions Fe3+ and Cr3+ carrying spin-only moments of 5μB and 3μB, respectively. As can be seen from the cations' distribution of Table 2, the mixed spinel structure of this system having Cr3+ in their preferred B-sites and Fe3+ in both A and B-sites, would generate a net moment of ||MB − MA|| decreasing as Cr replaces Fe in B-sites only; where MA and MB are the anti-parallel moments of sub-lattice of A-site and B-site, respectively. This is in accordance with Neel's two sub-lattice crystal field model of

ferrites [39, 40]. In this respect, HC and MR decrease with Cr content could also be due to exchange interaction between different magnetic characters of hard sub-lattice A and soft sub-lattice B.

Measured saturation magnetizations MS against temperature T for all compositions are shown in Fig. 4. The black symbols above 300 K represent the data obtained by VSM measurements and the red symbols below 300 K represent the data obtained by SQUID measurements. As can be seen from Fig. 4, the magnetizations have been largely saturated at a field of 22 kOe. Our data values at 300 K and saturating fields for compositions MgFe2O4 and MgCr0.5Fe1.5O4 are in good agreement with those of Anjum et al. [32] and Kumar et al. [41] but less good for compositions MgCr0.7Fe1.3O4 and MgCrFeO4 with those of Hankare et al. [33] and Raghasudha et al. [42]. The most striking feature of Fig. 4 curves is their gradual change in their decrease rate with temperature. Indeed, pure Mg ferrite MgFe2O4 appears to be magnetically the hardest compared to other compositions, i.e. it shows a slow MS diminution with temperature. This is evident because of the strong magnetic moments (5μB) of Fe3+ cations located in both A- and B-sites as well as the non-magnetic cations Mg2+ in both A- and B-sites. Then, as Cr3+ smaller moments (3μB) substitute Fe3+, the ferrite tends to gradually become magnetically soft by presenting a faster decrease of MS in the low temperature region. For example, curve of sample x = 0.5 appears to be steeper than the one of x = 0.2, and that of sample x = 1 is much steeper than x = 0.7. This aspect is confirmed by the monotonic decrease of HC and MR with chromium content as observed in Fig. 3 inset. Similar shapes of MS versus T curves have been reported on Ni–Cr [23] and Mg–Al ferrites [21].

Fig. 4

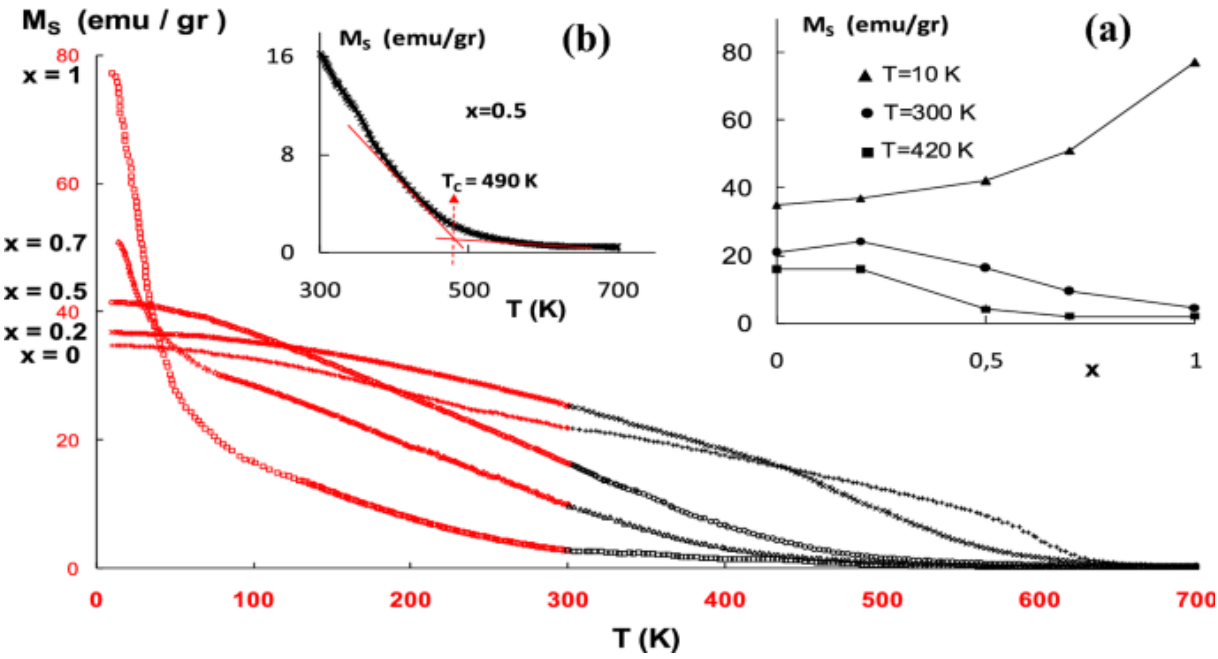

Saturation magnetizations MS versus temperature T of ferrites MgCrxFe2−xO4 at different chromium content: x = 0, 0.2, 0.5, 0.7 and 1. The black symbols are the VSM measurements and the red symbols are the SQUID measurements. Insets: a saturation magnetizations MS versus x for three temperatures 10 K, 300 K and 420 K; b representative curve of MS versus T at composition x = 0.5

In the inset (a) of Fig. 4 are depicted the saturation magnetizations (MS) versus chromium content x for three different temperatures: 420 K, 300 K and 10 K. At high temperatures, MS decreases monotonically with x, at intermediate temperature (300 K), it presents a peak for x = 0.2. Moreover, it is worth noting that this non-linear trend of MS versus cations content of ferrites is common and has been observed by Yadav et al. [43] on Co–Mn ferrites, by Haque et al. [44] on Mg–Zn ferrites and by Chirawatkul et al. [45] on Co–Mg. The most interesting part is the low temperatures region, more precisely the lowest values at 10 K, where we observe a sharp increase of MS with increasing x from 0 to 1. This is consistent with Néel's two sub-lattice model as we will discuss further for temperatures near 0 K.

The Curie temperatures, TC, were extracted from magnetization versus temperature curves using the standard method of "intersecting tangents" [40]. It consists of drawing two tangents on the curve to either side where the magnetic-paramagnetic transition appears to occur, the intersection of the two tangents is at TC. Inset (b) of Fig. 4 shows a representative curve of MS versus T over 300 K to 700 K range and the intersecting tangents at Curie temperature TC, for chromium content x = 0.5. Figure 5 and Table 3 show the Curie temperatures TC against chromium concentration x. A reasonable agreement has been found with the data of Nesa et al. [46] at x = 0 up to 1, but less good with Haque et al. [44] and Franco et al. [36]. A relative error of less than 4% was estimated from the uncertainty in drawing the tangents, in this respect, it is difficult to assert whether the trend is linear but it obviously shows decreasing TC with increasing x. It has been found that the Curie temperature of magnetic oxides having ideal chemical composition are closely related to the number of Fe3+–O2––Fe3+ bonds per Fe3+ ion per formula unit and also on their distribution over the A and B sites [23, 24]. The chains of such bonds are indefinitely long in a crystal of ideal chemical composition. However, when iron ions are reduced in number due to substitutions by Cr3+ ions, the number of active bonds decreases and there is a weakening of the A–B exchange interaction. The bonding energies necessary to offset the spin alignment will decrease and the Curie temperature is expected to fall. Similar trend of TC versus composition has been reported for Mg–Zn [44] and Li–Cr [24] ferrites.

Fig. 5

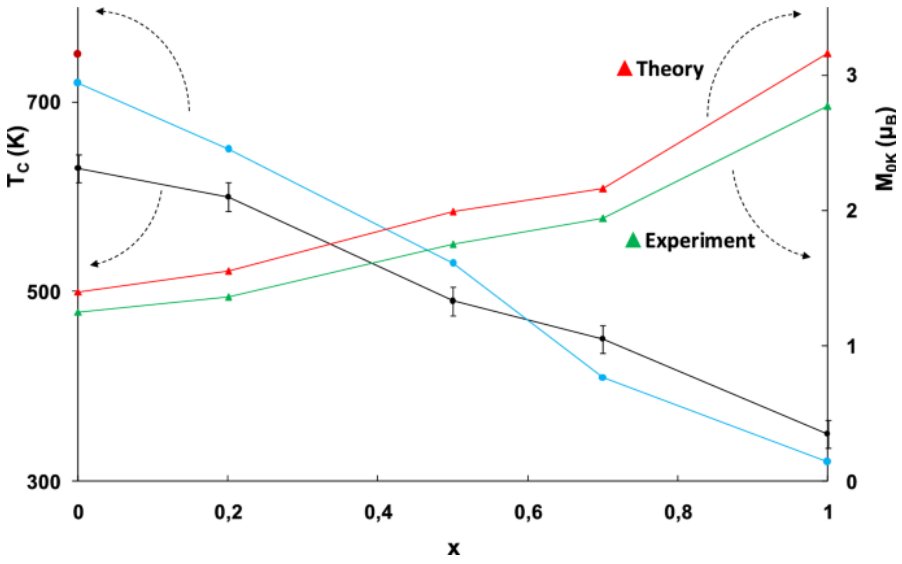

Curie temperatures TC versus chromium content x including data of Ref. [40] in blue and Ref. [42] in brown. Theoretical and experimental magnetic moments M0K (μB) at 0 K in Bohr magnetons μB per formula unit

SQUID measurements

The saturation magnetizations obtained by SQUID measurements of all compositions are plotted against T3/2 and T2 over an extended range of temperatures as shown in Fig. 6a and b, respectively. They are fitted to Bloch functions: MS(T) = MS(0) + const. T3/2 and MS(T) = MS(0) + const. T2 [47]. Moreover, in the more exact formula of Dyson [48], there are other terms containing T5/2 and T3 depending on the involved exchange interactions. Hence, the T3/2 and T2 Bloch functions are extrapolated linearly to 0 K as shown in Fig. 6 and both laws give almost the same values of MS(0) at 0 K with an uncertainty of less than 4%. Then, these extrapolated values are used to determine the experimental magnetic moments in Bohr magnetons μB per chemical formula unit M0K (μB) at 0 K using the following formula [23, 24]:

M0K(μB)=molarweight×MS/5585

Fig. 6

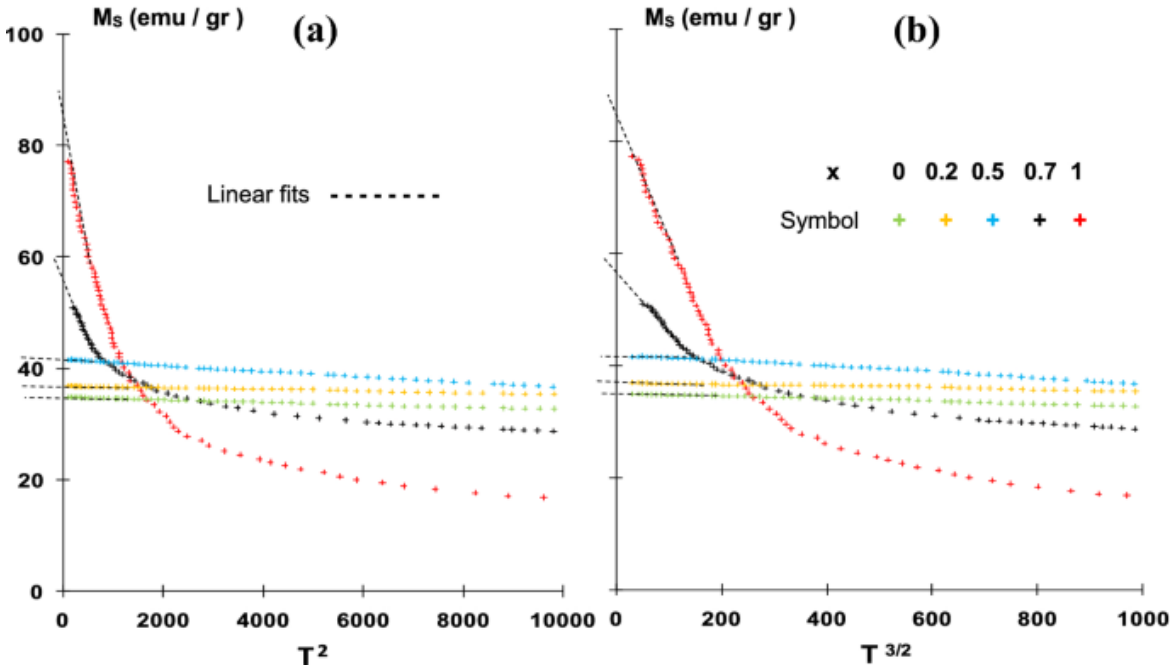

Block functions MS of T2 and T3/2, over low temperature range: a MS(T) = MS(0) + const. T2 and b MS(T) = MS(0) + const. T3/2; for different chromium content x = 0, 0.2, 0.5, 0.7 and 1. MS(0) are extracted by extrapolation to 0 K from the linear fits in dotted lines

Table 2 shows the experimental magnetic moments M0K (μB) obtained by linear extrapolation of T3/2 and T2 Block function laws.

From Néel's two sub-lattices crystal field model, the theoretical magnetic moments M0K (μB) in Bohr magnetons per formula unit at 0 K were calculated from sub-lattice moments MA and MB of A and B sites, respectively, i.e. M0K (μB) = ||MB − MA||, using the cations' distribution (Table 2) obtained by Rietveld refinement and the spin-only values of Fe3+ (5μB) and Cr3+ (3μB) assuming a weak spin–orbit coupling of atoms [1, 40]. The theoretical and experimental results are shown in Table 2 and their variations with chromium concentration are depicted in Fig. 5. It is interesting to point out the almost linear increase of both theoretical and experimental M0K (μB) with Cr content x though their magnitude are far apart. Note that this trend was not observed in MS values neither at room nor at high temperature (Fig. 4 inset a), which suggests that exchange coupling in this system is essentially governed by the intra-sub-lattice interactions as well as inter-sub-lattices interactions. This is based on the fact that doping would result in significant changes of the intra-site interactions due to preferential site occupancy of Cr3+ ions in B-sites only as argued by several workers [49,50,51] and keeping this system in the same mixed spinel structure from x = 0 up to x = 1. The inconsistency of magnetic moments values between theory and experiment is an inter-play of several reasons; one of them could be the effect of canted spins within the same sub-lattices A or B as developed by Yafet and Kittel [52] in an extended Néel's model. Indeed, in addition to the collinear ferrimagnetic structure described here, a so-called triangular structure of moments can take place. In this case, the total energy is lower when some of the ionic magnetizations make an angle with each other that differs from 0° to 180°. Yafet and Kittel suggested that, where the A–A and B–B interactions are not small compared with A–B, the A and B sub-lattices can be split further into A1 and A2, B1 and B2. Non-collinear angles occur between the magnetization vectors within A and B, but the resultant magnetizations of A and B are still antiparallel.

Conclusion

This study of the cations' distribution obtained by Rietveld refinement of MgCrxFe2−xO4 ferrites and their magnetic properties reveals that:

1.

The crystalline structure is a partially inversed spinel over the whole range of concentration from x = 0 to x = 1.

2.

At room temperature, the coercitive field and remanence decrease with chromium content.

3.

The saturation magnetization variation with chromium content is non-linear at 300 K, but shows a monotonic increase at 10 K.

4.

The Curie temperature decreases monotonically with the substitution of iron by chromium.

5.

The magnetic moments at 0 K calculated using cations' distribution consistent with Rietveld refinement analysis show an increasing trend with chromium content. This trend agrees with magnetic measurements.

References

1. B.D. Cullity, C.D. Graham, Introduction to Magnetic Materials,

2nd edn. (Wiley, NewJersey, 2009)

2. E.W. Gorter, Magnetization in ferrites: saturation magnetization

of ferrites with spinel structure. Nature 165, 798–804 (1950)

3. J. Crangle, Solid State Magnetism (Edward Arnold Pub. Co.,

London, 1991)

4. S. Mazen, N.I. Abu-Elsaad, A.S. Nawara, Infuence of divalent

metal ions substitution on the structural and magnetic properties

of Ni-Zn spinel ferrite. Phys. Sol. State 62, 1183–1194 (2020)

5. J. Smith, H.P. Wijn, Spinel Ferrites (Philips Tech. Lib., Eindhoven (Holland, 1959)

6. H. Knoch, H. Dannheim, Temperature dependence of the cation distribution in magnesium ferrite. Phys. Stat. Sol. (A) A37,

K135–K137 (1976)

7. H. Nikmanesha, M. Eshraghib, S. Karimi, Cation distribution,

magnetic and structural properties of CoCrFe2O4: efect of

calcination temperature and chromium substitution. J. Magn.

Magn. Mater. 471, 294–303 (2019)

8. L. Kumar, P. Kumar, A. Narayan, M. Kar, Rietveld analysis of

XRD patterns of diferent sizes of nanocrystalline cobalt ferrite

International. Nano Let. 38, 1–12 (2013)

9. A.S. Kamzin, A.A. Valiullin, A. Bingolbali, N. Dogan, Structural transformations of Ni1−xCuxFe2O4 nanoparticles depending on copper ions. Phys. Sol. State 62, 1231–1239 (2020)

10. Q.A. Pankhurst, J. Connolly, S.K. Jones, J. Dobson, Application

of magnetic nanoparticles in biomedicine. J. Phys. D 36, R167

(2003)

11. R. Jurgons, C. Seliger, A. Hilpert, L. Trahms, S. Odenbach,

C. Alexiou, Drug loaded magnetic nanoparticles for cancer

therapy. J. Phys.: Condens. Matter 18, S2893 (2006)

12. J. Philip, P.D. Shima, B. Raj, Iron oxide nanofuids and study of

temperature dependence of thermal conductivity and viscosity.

Appl. Phys. Lett. 92, 043108 (2008)

13. P. Tailhades, C. Bonningue, A. Rousset, L. Bouet, I. Pasquet, S.

Lebryun, Tailoring phase, microstructure and magnetic properties of nano cobalt ferrite. J. Magn. Magn. Mater. 193, 148

(1999)

14. M.Y. Yang, S. Seong, E. Lee, M. Ghanathe, A. Kumar, S.M.

Yusuf, Y. Kim, J.S. Kang, Electronic structures and magnetization reversal in Li0,5FeCr1,5O4. Appl. Phys. Lett. 116, 252401–

252405 (2020)

15. R.S. Getso, J. Mohammed, G. Mukhtar, N. Halilu, S. Sharma,

A.K. Srivastava, M. Ahmad, D. Basandrai, Structural and

dielectric properties of Cr substituted cobalt ferrites. J. Phys.:

Conf. Ser. 1531, 12029 (2020)

16. K. Seshan, A.L. Shashimohan, D.K. Chakrabarty, A.B. Biswas,

Efect of cation distribution on the properties of some magnesium-nickel ferrites. Phys. Status Solidi (A) 68, 97–101 (1981)

17. S. Hossain, M.K. Hasan, S.M. Yunus, A.K.M. Zakaria, T.K.

Datta, A.K. Azad, Synthesis and investigation of the structural

properties of Al doped Mg ferrites. Appl. Mech. Mater. 789,

48–52 (2015)

18. A.A. Pandit, A.R. Shitre, D.R. Shengule, K.M. Jadav, Efect of

Cd2+ doping on structural and magnetic properties of magnesium

ferrites. J. Mater. Sci. 40, 423 (2005)

19. S. Raghuvanshi, P. Tiwari, S.N. Kane, D.K. Avashi, F. Mazaleyrat,

T. Tatarchuk, I. Mironyuk, Dual control on structure and magnetic

properties of Mg ferrite. J. Magn. Magn. Mater. 471, 521–528

(2019)

20. M. Raghasudha, D. Ravinderb, P. Veerasomaiah, Electrical resistivity studies of Cr doped Mg nano-ferrites. Mat. Discov. 2, 50–54

(2015)

21. S. Hossain, M.K. Hasan, S.M. Yunus, A.K.M. Zakaria, T.K. Datta,

A.K. Azad, Synthesis and investigation of the structural properties

of Al3+ doped Mg ferrites. Appl. Mech. Mat. 789, 48–52 (2015)

22. M.B. Mohamed, M. Yehia, Cation distribution and magnetic

properties of nanocrystalline gallium substituted cobalt ferrite. J.

Alloys Comp. 615, 181–187 (2014)

23. A. Rais, A.M. Gismelseed, I.A. Al-Omari, Cation distribution and

magnetic properties of nickel–chromium ferrites NiCrxFe2−xO4.

Phys. Stat. Sol. (B) 242(7), 1497–1503 (2005)

24. A. Rais, A.M. Gismelseed, I.A. Al-Omari, On the magnetic compensation efect of lithium-chromium ferrites Li0.5CrxFe2.5−xO4.

Phys. Stat. Sol. (B) 242(14), 2949–2955 (2005)

25. K. Sabri, A. Rais, K. Taibi, M. Moreau, B. Ouddane, A.

Addou, Structural Rietveld refnement and vibrational study of

MgCrxFe2−xO4 spinel ferrites. Physics B 501, 38–44 (2016)

26. N. Bouhadouza, A. Rais, S. Kaoua, M. Moreau, K. Taibi, A.

Addou, Structural and vibrational studies of NiAlFe2O4 ferrites.

Ceram. Int. 41, 11687–11692 (2015)

27. R.Y. Young, The Rietveld Method, 3rd edn. (Oxford University

Press, Oxford, 1996)

28. B.D. Cullity, S.R. Stock, Elements of X-ray Difraction, 3rd edn.

(Pearson New Int, USA, 2013)

29. R.A. Young, D.B. Wiles, Profle shape functions in Rietveld

refnements. J. Appl. Cryst. 15, 430–438 (1982)

30. C. Suryanarayana, M. Nortan, X-ray Difraction: A Practical

Approach (Plenum Publishing Corporation, NewYork, 1998)

31. K.E. Sickafus, J.M. Wills, N.W. Grimes, Structure of spinel. J.

Am. Ceram. Soc. 82, 3279–3292 (1999)

32. S. Anjum, M. Pervaiz, A. Rashid, R. Rehana, Investigation of

cationic distribution, magnetic and dielectric properties of Crsubstituted Mg ferrites. J. Electron. Mater. 48, 806–816 (2019)

33. P.P. Hankare, V.T. Vadera, N.M. Patil, S.D. Jadhava, U.B. Sankpala, M.R. Kadama, B.K. Chouguleb, N.S. Gajbhiyec, Synthesis, characterization and studies on magnetic and electrical

properties of Mg ferrite with Cr substitution. Mater. Chem.

Phys. 113, 233–238 (2009)

34. M. Raghasudha, D. Ravinder, P. Veerasomaiah, Electrical and

magnetic properties of Mg-Cr and Co-Cr nano- ferrites synthesized by citrate-gel method. Sol. State Phenom. 241, 69–92

(2016)

35. G. Vaidyanathana, R. Arulmurugana, S.D. Likhiteb, M.R. Anantharamanc, M. Vaidyad, N.D. Senthilrama, Efect of preparation

on magnetic properties of Mn-Zn ferrite. Ind. J. Eng. Mater. Sci.

11, 289–294 (2004)

36. A. Franco, M.S. Silva, High temperature magnetic properties

of magnesium ferrite nanoparticles. J. Appl. Phys. 109, 07B505

(2011)

37. F. Safari, P. Kamelin, M. Rahimi, H. Ahmadvand, H. Salamati,

Efects of Co-substitution on the structural and magnetic properties of NiCoxFe2−xO4 ferrite nanoparticles. Ceram. Int. 41, 7352–

7358 (2015)

38. S. Maensiri, M. Sangmanee, A. Wiengmoon, Magnesium ferrite (MgFe2O4) nanostructures fabricated by electrospinning.

Nanoscale Res. Lett. 4, 221–228 (2009)

39. L. Néel, Propriétés magnétiques des ferrites; ferrimagnétisme et

antiferromagnétisme. Ann. Phys. 3, 137–198 (1948)

40. D. Jiles, Introduction to Magnetism and Magnetic Materials

(Chapman and Hall Ltd., London, 1991)

41. D.R. Kumar, S.I. Ahmad, Ch. Abraham Lincoln, D. Ravinder,

Structural, optical, room-temperature and low temperature magnetic properties of Mg–Zn nanoferrite ceramics. J. Am. Ceram.

Soc. 7, 53–68 (2019)

42. M. Raghasudha, D. Ravinder, P. Veerasomaiah, Investigation of

superparamagnetism in MgCr0.9Fe1.1O4 nano-ferrites synthesized

by the Citrate-gel method. J. Magn. Magn. Mater. 355, 210–214

(2014)

43. S.P. Yadav, S.S. Shinde, P. Bhatt, S.S. Meena, K.Y. Rajpure, Distribution of cations in CoMnFe2O4 using XRD, magnetization and

Mossbauer spectroscopy. J. Alloys Comp. 646, 550–556 (2015)

44. M.M. Haque, M. Huq, M.A. Hakim, Efect of Zn2+ substitution

on the magnetic properties of MgZnFe2O4 ferrites. Physics B 404,

3915–3921 (2009)

45. P. Chirawatkul, S. Khoonsqp, S. Phumying, C. Kaewhan, S. Pinitsoontorn, S. Maensiri, Cation distribution and magnetic properties

of CoMgFe2O4. J. Alloys Comp. 697, 249–256 (2017)

46. F. Nesa, A.K.M. Zakaria, M.A. Saeed Khan, S.M. Yunus, A.K.

Das, S.G. Eriksson, M.N.I. Khan, D.K. Saha, M.A. Hakim, Structural and magnetic properties of Cr-Mg ferrites. J. Cond. Mater.

Phys. 2, 27–35 (2012)

47. U. Kobler, A. Hoser, Sol. State Commun. 142, 35014 (2007)

48. F.J. Dyson, Phys. Rev. 102, 1230 (1956)

49. A.K.M. Zakaria, M.A. Asgar, S.G. Eriksson, F.U. Ahmed, S.M. Yunus, H. Rundlof, The study of magnetic ordering in the spinel system ZnxNi1−xFeCrO4 by neutron difraction. J. Magn. Magn. Mater. 265, 311–320 (2003)

50. V.D. Murumkar, K.B. Modi, K.M. Jadhav, G.K. Bichile, R.G. Kulkarni, Magnetic and electrical properties of aluminium and chromium co-substituted titanium ferrite. Mater. Lett. 32, 281 (1997)

51. W.A. Bayoumya, M.A. Gabalb, Synthesis characterization and magnetic properties of Cr-substituted NiCuZn nanocrystalline ferrite. J. Alloys Comp. 506, 205–209 (2010)

52. Y. Yafet, C. Kittel, Antiferromagnetic arrangements in ferrites. Phys. Rev. 87, 290 (1952)